

RESEARCH PAPER



## MicroRNA signature in the chemoprevention of functionally-enriched stem and progenitor pools (FESPP) by Active Hexose Correlated Compound (AHCC)

Émilie A. Graham<sup>a</sup>, Jean-François Mallet<sup>b</sup>, Majed Jambi<sup>b</sup>, Hiroshi Nishioka<sup>c</sup>, Kohei Homma<sup>c</sup>, and Chantal Matar<sup>a,b</sup>

<sup>a</sup>Interdisciplinary Health Sciences, University of Ottawa, Ottawa, Canada; <sup>b</sup>Cellular and Molecular Medicine, Faculty of Medicine, University of Ottawa, Ottawa, Ontario, Canada; <sup>c</sup>R&D Division Amino Up Chemical Co, Ltd, Sapporo, Japan

### ABSTRACT

**Purpose:** Many breast cancer patients use natural compounds in their battle against breast cancer. Active Hexose Correlated Compound (AHCC<sup>®</sup>) is a cultured mushroom mycelium extract shown to favorably modulate the immune system and alleviate cancer burden. Cancer Stem cells (CSCs) are a subset of highly tumorigenic cancer cells that are thought to be responsible for recurrence. CSCs can be epigenetically regulated by microRNAs (miRNAs). We hypothesized that AHCC may influence CSCs by modulating tumor-suppressor or oncogenic miRNAs. **Methods:** Functionally-enriched stem and progenitor pools (FESPP) were isolated in the form of mammospheres from MDA-MB-231, MCF-7, and 4T1 cells, exposed to AHCC in both regular and primary culture from Balb/c mice, and analyzed by visual counting and flow cytometry. Cell motility was also observed in MDA-MB-231 cells. Profiling and RT-qPCR were performed to determine AHCC influence on miRNAs in MDA-MB-231 mammospheres. Additionally, Balb/c mice were orally gavaged with AHCC, and tumor growth parameters and miR-335 expression were analyzed. MDA-MB-231 cells were transfected with miR-335 and analyzed by western blot. **Results:** We demonstrated that AHCC reduced mammosphere growth in three cell lines and in primary culture, prevented cell migration, and upregulated miR-335 expression in MDA-MB-231 cells and mouse tumor samples. Among the differentially regulated miRNAs in CSCs, we focused on tumor suppressor miR-335, known to target extracellular matrix protein Tenascin C (TNC). TNC is involved in CSC immune evasion pathways. In MDA-MB-231, inhibition of miR-335 increased TNC protein expression. **Conclusions:** These results support that AHCC limits FESPP growth, partly by targeting miRNA pathways.

**Abbreviations:** AHCC, Active Hexose Correlated Compound; CAM, Complementary and alternative medicine; CSC, Cancer stem cell; EMT, Epithelial-mesenchymal transition; FESPP, Functionally-enriched stem and progenitor pools; NK, Natural killer cell; TNBC, Triple negative breast cancer; TNC, Tenascin C

### ARTICLE HISTORY

Received 10 June 2016  
Revised 25 July 2017  
Accepted 24 August 2017

### KEYWORDS

AHCC; breast cancer; cancer stem cell; microRNA; Tenascin C

### Introduction

Currently, there is considerable interest in nutritional interventions and natural compounds for targeting key deregulated niche signaling pathways in tumor development. For example, a dietary intervention showed that a few months of Mediterranean diet was sufficient to positively change the metabolic/endocrine characteristics of breast cancer survivors.<sup>1</sup> More specifically, the naturally derived product Active Hexose Correlated Compound (AHCC<sup>®</sup>), from the culture of Basidiomycete mushroom extract, has been reported to exert immunoprotective effects against many types of cancer, including liver, breast, colon and prostate.<sup>2–5</sup> It is thought that the active components in AHCC are its acylated  $\alpha$ -1,4 glucans.<sup>6</sup> Further, it has been shown to increase the activity of immune cells in clinical studies<sup>7,8</sup> and enhance the antitumor effects of certain chemotherapy drugs in<sup>5</sup> and have anti-inflammatory effects in animal studies.<sup>9</sup>

The pathological growth of tumors is maintained and driven by a small subpopulation of “stem-like” tumor cells, ensuring

resistance to both chemotherapy and radiation.<sup>10–14</sup> This highly tumorigenic subset of breast cancer cells display increased ability to self-renew, generate breast cancer heterogeneity, and are designated Cancer Stem Cells (CSCs).<sup>15</sup> In breast cancer, CSCs can be isolated by the CD44<sup>+</sup>/CD24<sup>-</sup> phenotype and by their ability to grow as spheres known as mammospheres<sup>16–18</sup> CSCs are believed to be connected to the epithelial-mesenchymal transition (EMT), which is associated with metastasis as it allows cells to migrate and invade nearby tissues and enter the bloodstream.<sup>19</sup>

The oncogenic Tenascin C (TNC), is an extracellular matrix protein that is expressed in breast cancer cells and is negatively associated with T cell migration.<sup>20,21</sup> It has been shown to be highly expressed during tissue repair and embryonic development, as well as in chronic inflammation and cancer<sup>22–26</sup> TNC promotes the expression of stem cell signaling components involved in EMT pathways and is needed for the activation of the Wnt/ $\beta$ -catenin signaling pathway in the stem cell niches, allowing for the maintenance of the stem cell pool.<sup>21,27</sup> CSCs have been shown to

avoid immune surveillance through the TNC- $\alpha 5\beta 1$  axis.<sup>28</sup> This immune evasion may be one explanation for CSC survival and tumor recurrence.

CSCs are subject to epigenetic regulation, particularly by the expression of microRNAs (miRNAs); small, noncoding RNAs that have emerged as critical regulators of CSC functions in cancer initiation, therapy resistance and metastasis.<sup>29</sup> Recent studies have shown that natural agents can alter miRNA expression profiles.<sup>30</sup> miRNAs are often over-expressed or down-regulated in a number of malignancies<sup>31</sup> and some can also function as tumor suppressors or as oncogenes.<sup>32</sup> In particular, miR-335 is down-regulated in breast cancer, especially in patients with BRCA mutations.<sup>33</sup> It has also been implicated in modulating several protein pathways<sup>34–37</sup> including suppressing metastasis and migration by inhibiting TNC expression.<sup>36</sup> Additionally, miR-335 was found to be down-regulated in CSCs and to inhibit CSC growth.<sup>38</sup> These studies demonstrate that miR-335 is a promising target in breast cancer stem cells.

Therefore, we propose that AHCC targets CSCs through epigenetic mechanisms, such as through changing the expression of microRNAs, such as miR-335, and indirectly inhibiting Tenascin C protein expression. We investigated these effects in three different cell lines, with a focus on a TNBC cell line, and in Balb/c mice.

## Methods

### AHCC preparation

AHCC was obtained from the Amino Up Chemical Co., Ltd. (Sapporo, Japan). We prepared 40 mg/ml AHCC in DMEM-F12 and filtered it through a 0.22  $\mu$ m Millex-GV filter.

### Cell culture and mammosphere growth

MDA-MB-231 and 4T1 cell lines were cultured in RPMI 1640 (1X) and MCF-7 cells were cultured in DMEM (1X) (Gibco, Grand Island, NY, USA). All cells were incubated at 37°C and 5% CO<sub>2</sub>. Adherent cells were detached by trypsin and single cells were counted using the Countess automated cell counter (Invitrogen, Burlington, ON). Afterwards, the cells were plated on Costar ultra-low attachment plates (Corning, St. Laurent, QC) in spheroid medium. Spheroid medium consists of DMEM-F12 (Invitrogen) combined with 100mM Sodium pyruvate, 250 mM L-glutamine (Sigma Aldrich, Oakville, ON), 100  $\mu$ g/mL hydrocortisone (Sigma Aldrich), 1000x streptomycin-penicillin (Sigma Aldrich), 20  $\mu$ g/mL bFGF, 20  $\mu$ g/mL EGF, and 10 mg/mL insulin.  $2 \times 10^4$  cells/ml were plated in 96-well ultra-low attachment plates and  $2 \times 10^5$  cells/ml (for a 24 h extraction) or  $3 \times 10^5$  cells/ml (for a 5 h extraction) were plated in 6-well ultra-low attachment plates. Mammospheres were exposed to 0–4 mg/ml AHCC in treatment group. Mammospheres were counted in the 96-well ultra-low attachment plates by light microscopy and miRNA were extracted from mammospheres in 6-well ultra-low attachment plates after 5 hours and at least 3 samples were used in each analysis.

### Flow cytometry

Three samples of mammospheres from MDA-MB-231 were collected after 24h, washed with phosphate-buffered saline (PBS) and then enzymatically dissociated with 0.05% trypsin/0.25% EDTA into single cell suspension. Combinations of monoclonal antibodies against human cell, CD44-APC (BD Biosciences) and CD24-PE/CY7 (eBioscience), were added to the cell suspension at concentrations recommended by the manufacturer and incubated at 4°C in the dark for 30 to 40 minutes. For all mammospheres, labeled cells were washed with PBS to eliminate unbound antibody, and the flow cytometry was analyzed on a BeckmanCoulter MoFlo XDP (San Francisco, CA, USA). Dead cells were eliminated by using the viability dye DAPI. Side scatter and forward scatter profiles were used to eliminate cell doublets. A minimum of 10,000 events were recorded for each sample.

### Cell viability and proliferation

Three samples of MDA-MB-231 cells were grown in a 96-well plate at a concentration of  $2 \times 10^5$  cells/ml in RPMI medium with FBS, streptomycin and penicillin. The cells were then exposed to concentrations of 0–8 mg/ml AHCC for 24 hours. The MTT-based *In Vitro* Toxicology Assay Kit (Sigma-Aldrich) and the protocol was followed with an incubation period of 4 hours.

### Cell motility

Three samples of MDA-MB-231 cells were plated in a 6-well Corning tissue culture treated plate at a concentration of  $3 \times 10^5$  cells/ml and exposed to 0–4 mg/ml of AHCC for 24 hours at 37°C and 5% CO<sub>2</sub>. A scratch was then made with a 1000 $\mu$ l pipette tip and photographs were taken at 0 hours, 24 hours, and 48 hours or 72 hours.

### MicroRNA profiling

MDA-MB-231 mammospheres were extracted 24 hours after plating. The two treatment group samples were exposed to 4 mg/ml of AHCC for 24 hours and the two control group samples were given an equal volume of medium. Sample purity and integrity were verified with a NanoDrop 2000 (Thermo Scientific, Waltham, MA, USA) and Agilent 2100 BioAnalyzer (Bio-Rad, Hercules, CA, USA), respectively. Microarray analysis was completed by an Affymetrix GeneChip<sup>®</sup> miRNA 3.0 Array

### Real-time quantitative reverse transcription PCR

After 5 hours of exposure to AHCC or control conditions, three samples of cancer stem cells were extracted using the miRNeasy mini kit (Qiagen, Toronto, ON). Then, the samples underwent a reverse transcription reaction to form cDNA by using individual probes. The cDNA was synthesized by Moloney Murine Leukemia Virus (MMLV) Reverse Transcriptase (Invitrogen). The expression of snRNA-U6, and target miR-335, was measured by RT-qPCR using TaqMan probes (Applied Biosystems, Burlington, ON) and a

FastStart Taq Polymerase (Roche, Mississauga, ON) in a CFX96 machine (Bio-Rad).

### Transfection

MDA-MB-231 cells were allowed to grow to 30% confluence in RPMI medium with FBS and antibiotics in 15ml flasks. The cells were then incubated with Lipofectamine (Life Technologies, Burlington, ON) and the targets: mirVana™ non-coding negative control 1, miR-335 mimic (ID: MH10063), and miR-335 inhibitor (ID: MH10063) (Ambion, ThermoFisher Scientific) for 48 hours. After incubation, a passage was completed and cells were plated in regular 6-well plates or ultra-low attachment. MicroRNA were then extracted, reverse transcribed, and analyzed by RT-qPCR.

### Protein analysis

Three samples of MDA-MB-231 cells were transfected for 48 hours in a 6 well attachment plate and extracted. Cells were washed with PBS on ice and then mixed with 300 ul Pierce® RIPA buffer (Thermo Scientific) combined with the Halt™ Protease and Phosphatase Inhibitor Cocktail (100X) (Thermo Scientific). Cells were then scraped off the plate and protein samples were centrifuged to remove the outer membrane. Protein concentrations were quantified by the BCA Protein Assay Kit (Pierce). Samples were prepared in Laemmli sample buffer, heated for 5 min at 95°C and loaded on precast Bolt® Bis-Tris Plus Gels (Invitrogen). The electrophoresis was carried in MES buffer (Invitrogen) at 200 volts in a Mini Gel Tank (Life Technologies). The gels were transferred to Immobilon-p50 PVDF membranes in a Trans-Blot Cell (Bio-Rad). The membranes were exposed to primary antibodies Anti-Tenascin C at a dilution of 1:2500 (Abcam ab108930, Cambridge, United Kingdom). The secondary antibody was a goat anti-rabbit used as a 1:10000 dilution (Jackson ImmunoResearch Laboratories, West Grove, PA, USA). Membranes were archived with a VersaDoc (Bio-Rad) and the intensity of each band was measured using Quantity One software (Bio-Rad).

### Mouse handling and feeding procedures

Thirty-one, six- to eight- week old Balb/c mice weighing between 18–20 g were obtained from Charles River (Montreal, QC, Canada). The mice were handled based on guidelines required by the Canadian Council on Animal Care and the experimental design was approved by the University of Ottawa Animal Care Committee under protocol ME-316. Mice were housed in plastic micro-insulators in a controlled atmosphere (temperature: 22 ± 2°C; humidity: 55 ± 2 %) on a 12-h light/dark cycle and fed a conventional balanced diet (2018 Teklad Global 18% Protein Rodent diet, Harlan Laboratories Inc, Madison, Wisconsin, USA) and water ad libitum. Eleven mice were gavaged with AHCC in 1% sucrose in water solution (1g/kg/day) for two weeks before tumor injection and 19–23 days following until sacrifice. The ten control group mice were gavaged with 1% sucrose in water solution instead. The ten mice saved for ex vivo studies were examined periodically following injection for stress that may have been caused

by tumor injection. All mice were injected with 1400 4T1 cells in the right abdominal mammary gland.

### Tumor extraction, measurement and mammosphere plating

Tumors were extracted based on the protocol described by Pulaski and Ostrand-Rosenberg<sup>39</sup> with a few minor changes. Tumors were weighed on a scale and measured with a caliper. For the ex vivo experiment, approximately 0.05 g of each tumor was minced and dissociated in RPMI-1640 media containing 300 U/ml collagenase (Sigma) at 37°C for 2 hours. Cells were sieved sequentially through a 40 μm cell strainer (BD Biosciences, San Diego, CA, USA) to obtain a single cell suspension. These cells were then counted using a Countess automated cell counter (Invitrogen, Burlington, ON) to determine concentration and viability. The cells were plated in ultralow attachment 96-well plates (Corning) at a concentration of  $2 \times 10^4$  cells/ml, in DMEM-F12 (Invitrogen), supplemented with 10 ng/ml EGF, 20 ng/ml bFGF, 5 μg/ml insulin, 1 mM sodium pyruvate, 0.5 μg/ml hydrocortisone, and penicillin/streptomycin (0.05 mg/mL) (Sigma). The mammospheres were exposed to concentrations of 0, 2, and 4 mg/ml of AHCC and examined at 24, 48, and 72 hours.

### Statistical analysis

Mammosphere growth in vitro and RT-qPCR results were analyzed by one-way ANOVA and post-hoc Tukey test, and ex vivo mammosphere growth and cell motility by two-way ANOVA on GraphPad Prism 5 (La Jolla, CA, USA). Flow cytometry results were analyzed with Kaluza 1.3 software (Beckman Coulter Inc., Montreal, QC). The cell motility assay was analyzed with TScratch software (CSE Lab, Zurich, Switzerland). Profiling results were analyzed with Mev 4.8.1 software, BRB Arraytools 4.4.0. The data was normalized using Robust Multichip Average (RMA).<sup>40</sup> The statistical analysis was done by a two-class unpaired SAM 1.0. Western blot analyses were conducted using Biorad Image Lab 5.2.1. Tumor volume and mass were analyzed by a student's t-test on GraphPad Prism 5.

## Results

### AHCC reduced mammosphere growth and size in vitro and ex vivo

A common procedure used to examine CSC growth is through the isolation and culturing of mammospheres, small congregations of FESPP suspended in the media.<sup>41</sup> Mammosphere growth was observed for 24 hours after exposure to AHCC in three cell lines: MDA-MB-231, 4T1, and MCF-7. A dose dependent effect was observed in all cell lines (Fig. 1a-c) and all ANOVA tests were found to be significant ( $p < 0.001$ ). Additionally, through observation, a reduction in mammosphere size was demonstrated in the three different cell lines (Fig. 1d). For ex vivo experiments, mice were injected with 4T1 cells for tumor extraction and mammosphere plating. Mammospheres exposed to AHCC grew significantly slower as compared to the

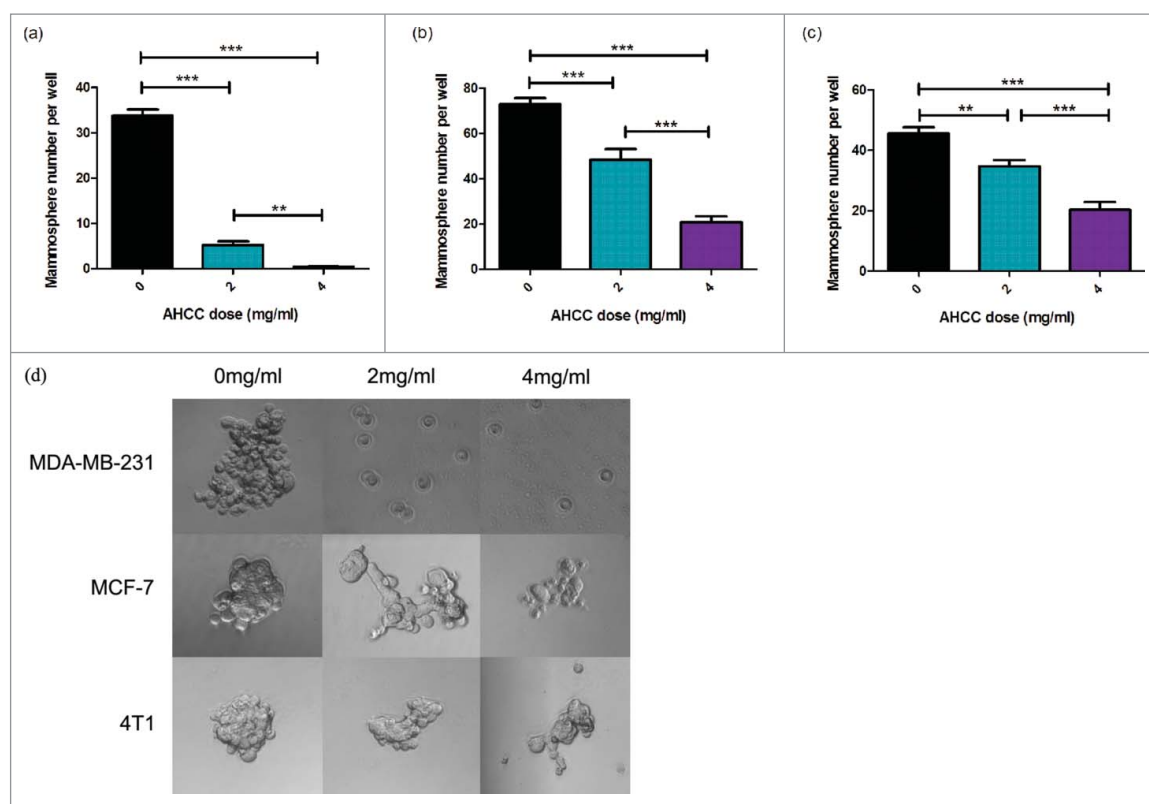


**Figure 1.** a-d. Mammosphere growth after AHCC exposure. (a) MDA-MB-231 mammosphere growth after 24 h exposure to AHCC. Approximately 3600 cells were added per well. Data is a combination of 6 experiments. (b) MCF-7 mammosphere growth after 24 h exposure to AHCC. Approximately 5100 cells were added per well. Data is a combination of 3 experiments. (c) 4T1 mammosphere growth after 24 h exposure to AHCC. Approximately 1700 cells were added per well. Data is a combination of 3 experiments. (d) Photographs of mammospheres taken with AxioCamMR3 camera on light microscope. Mammospheres were isolated and grown in a 96-well ultra-low attachment plate in DMEM-F12 and spheroid medium at 37°C and 5% CO<sub>2</sub>. All data are presented as mean ± SEM. Significance is represented by \*\* for  $p < 0.01$  and \*\*\* for  $p < 0.001$  by Tukey's post-hoc test.

control ( $p$ -value  $< 0.001$ ), but were not significantly different between doses (Fig. 2). An MTT assay demonstrated that AHCC had no significant toxicity on MDA-MB-231 mammospheres for a concentration of up to 8 mg/ml.

#### AHCC decreased the percentage of CD44<sup>+</sup>/CD24<sup>-</sup> phenotype cells in a MDA-MB-231 mammosphere population

Previous studies have shown that breast CSCs demonstrate a CD44<sup>+</sup>/CD24<sup>-</sup> phenotype with flow cytometry analysis.<sup>18</sup> Also, CD44 has previously been shown to predict the prognosis of TNBC, making it a useful marker for determining metastatic potential.<sup>42</sup> Flow cytometry analysis revealed an average of a 17.47% decrease of CD44<sup>+</sup>/CD24<sup>-</sup> phenotype cells (representing CSCs) after 24 hours of exposure to 4 mg/ml of AHCC, in comparison to the control (Fig. 3a-c). This further supports the mammosphere growth findings, suggesting that AHCC may target CSCs in breast cancer.

#### AHCC reduced MDA-MB-231 cell motility

We exposed attached MDA-MB-231 cells to AHCC over a 72 hour period. A reduction in cell motility was observed at 24 hours between the 4 mg/ml dose and control ( $p < 0.05$ ), and this difference significantly increased after 72 hours of AHCC exposure ( $p < 0.001$ ) (Fig. 4a-b). Samples were

additionally compared with the post hoc Tukey's Multiple Comparison Test. These results demonstrate that AHCC prevents cell motility in a TNBC cell line.

#### AHCC upregulated MiRNA-335 in MDA-MB-231 cells

The miRNA profiling revealed several miRNAs to be differentially expressed in MDA-MB-231 mammospheres exposed to AHCC in comparison to the controls. The miRNAs displayed were chosen based on whether they were a factor of 1.5 fold higher or lower in the AHCC group in comparison to the controls (Fig. 5). We chose to focus on miR-335 for its documented involvement in many types of cancer, including breast cancer.

To confirm these results, RT-qPCR analysis of miR-335 revealed an average of 3-fold higher miR-335 expression in MDA-MB-231 mammospheres when exposed to AHCC for 5 hours (Fig. 6). Although the profiling was completed after 24 hours of AHCC exposure, we determined that RT-qPCR performed at different time points revealed a more consistent fold change at 5 hours for miR-335. This suggests that AHCC may have early effects on miR-335 expression.

#### MiRNA-335 inhibition upregulated TNC protein expression in MDA-MB-231 cells

We performed a western blot analysis of MDA-MB-231 cells transfected with a mirVana<sup>TM</sup> miR-335 mimic or inhibitor or

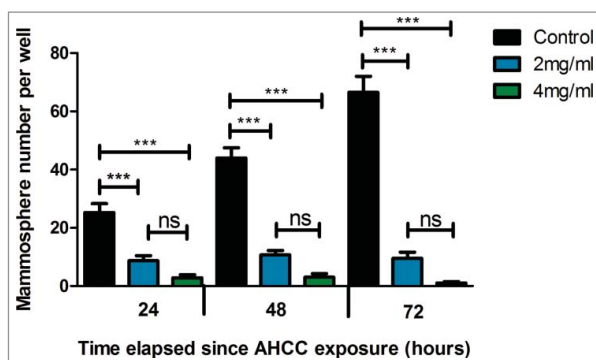


**Figure 2.** Ex vivo 4T1 mammosphere growth after 24, 48, and 72 hour exposures to AHCC. Data are expressed as mean  $\pm$  SEM. Mouse tumors were digested with collagenase and grown in 96-well ultra-low attachment plates at 37°C and 5% CO<sub>2</sub>. Approximately 3400 cells were added per well. Data is a combination of four mice. Significance is represented by \*\*\* for  $p < 0.001$  and non-significance by ns as calculated by Tukey's post-hoc test.

negative control 1. We found a relative increase in TNC protein expression with the addition of the miR-335 inhibitor (Fig. 7a-b). This suggests that miR-335 negatively regulated TNC in the TNBC cell line, MDA-MB-231. The mimic produced varying results and so these data were determined to be insignificant.

### AHCC upregulated miR-335 expression in mammary gland tumor cells

A downward trend was observed for tumor mass and volume measurements after the mice were gavaged with AHCC, however, no statistically significant difference was observed with the student T test. We also decided to examine the influence of AHCC on miR-335 in an *in vivo* setting by extracting it from the collected mouse tumors, and found a significantly higher expression of miR-335 in the AHCC group ( $p$ -value  $< 0.01$ ) (Fig. 8a-c). This finding supports that AHCC targets miR-335 in mammary gland tumor cells even after being subject to digestion and liver processing in the mice.

### Discussion

Naturally derived compounds have been shown to be effective in preventing and treating breast cancer. In fact, chemoprevention by targeting Cancer Stem Cells (CSCs) is an important paradigm in therapeutic and adjunct therapy in breast cancer. AHCC has proven to be effective in reducing tumor growth and metastasis in animal models, particularly when combined with a conventional therapy.<sup>5,43,44</sup> Therefore, we aimed to study

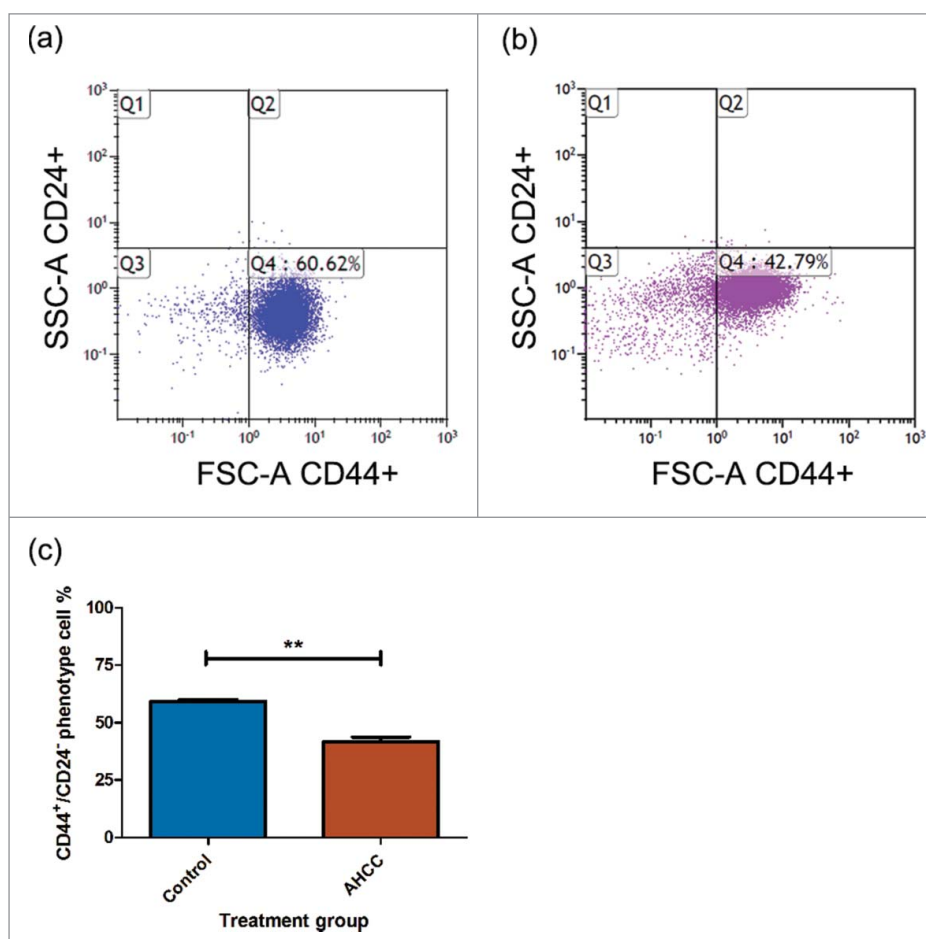


**Figure 3.** a-c. AHCC reduces CD44<sup>+</sup>/CD24<sup>-</sup> phenotype MDA-MB-231 cells. (a) Untreated MDA-MB-231 mammospheres. (b) Treated MDA-MB-231 mammospheres. The treatment group was exposed to 4 mg/ml of AHCC for 24 hours. (c) Comparison between untreated control and treated AHCC mammospheres with a combination of 3 experiments. Data are presented as mean  $\pm$  SEM. Significance is represented by \*\* for  $p < 0.01$  by Tukey's post-hoc test. MDA-MB-231 mammospheres ( $2 \times 10^5$  cells/ml) were plated in 6-well ultra-low attachment plates in DMEM/F12 and spheroid medium and incubated at 37°C and 5% CO<sub>2</sub>. The cells were exposed to antibodies CD44 and CD24 and profiles were analyzed by flow cytometry.

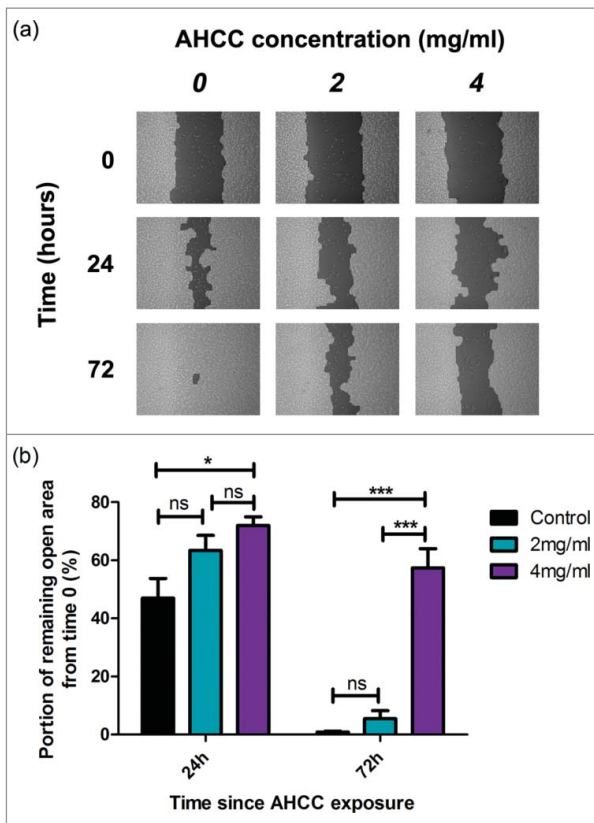


**Figure 4.** a-b. The influence of AHCC on MDA-MB-231 cell motility. (a) Photographs from TScratch program for one sample over a period of 72 hours. (b) Combined data from 3 experiments. Data are presented as mean  $\pm$  SEM. Significance is represented by \* for  $p < 0.05$  and \*\*\* for  $p < 0.001$  and non-significance by ns by Tukey's post-hoc test. Cells were grown to 90–100% confluence in a 6 well plate and scratched with a pipette tip down the middle of the well. Photos were taken on a light microscope.

the underlining mechanisms that drive the anti-carcinogenic effects of AHCC and its relationship to the Cancer Stem Cell Theory in Breast Cancer Stem Cells (BCSCs).<sup>45</sup> Since current therapies do not target CSCs, it is important to conduct research on possible alternative therapies.

Isolation of FESPP from cancer cell lines demonstrated that AHCC influenced mammosphere growth in a dose dependent manner, not only in MDA-MB-231 cells, but also in MCF-7 and 4T1 cells, suggesting that its effect is not cell type dependent (Fig. 1a-d). This was also confirmed by flow cytometry analysis (Fig. 3a-c). Although no other studies have examined the effects of AHCC on FESPP, it has previously been shown to target SOX2 and demonstrated cytotoxicity towards gemcitabine-resistant pancreatic cancer cells.<sup>46</sup> We similarly showed an effect on mammospheres cultured from Balb/c mice tumors, confirming that the effects also apply to primary culture (Fig. 2). Finally, we observed that AHCC prevents MDA-MB-231 cell migration (Fig. 4a-b). Together, these results indicate that AHCC inhibits FESPP growth and TNBC cell motility. This confirms that AHCC's anti-tumorigenic potential extends to breast cancer and may prevent recurrence by targeting CSCs within the FESPP, although future studies will need to truly isolate CSCs to confirm these findings. Since CSCs are known to be epigenetically regulated,<sup>47</sup> we decided to explore the effect of AHCC on miRNA profiling.

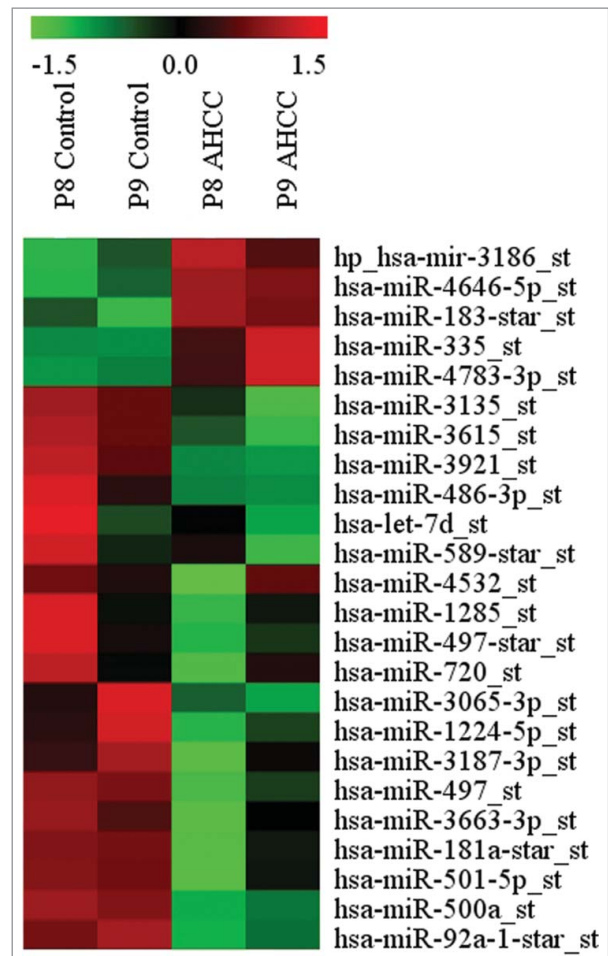


**Figure 5.** MicroRNAs differentially expressed in MDA-MB-231 after 24 h exposure to AHCC. The microRNAs were chosen based on whether their fold change was  $>$  or  $<$  by a factor of 1.5 in the AHCC group in comparison to the control. The profiling heat map represents a calculated z-score (-1.5 to 1.5 from mean). Each column and row represents a sample and specific miRNA expression, respectively. Columns are labeled as passage 8 (P8) or passage 9 (P9) for respective control and AHCC groups. AHCC concentration for this experiment was 4 mg/ml.

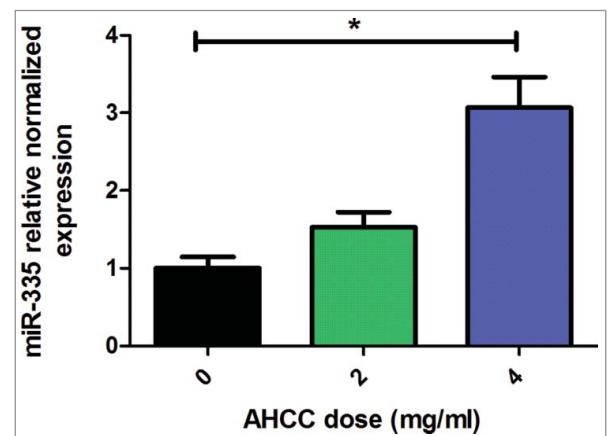


**Figure 6.** AHCC upregulates miR-335 expression in MDA-MB-231 mammospheres. Results are a combination of means  $\pm$  SEM from 3 separate experiments. MDA-MB-231 cells were plated in 6-well ultra-low attachment plates in DMEM-F12 and spheroid medium and incubated at 5% CO<sub>2</sub> and 37°C. Cells were exposed to varying concentrations of AHCC for 5 hours. MiR-335 expression levels were measured by RT-qPCR in comparison to reference snRNA U6. Significance is represented by \* for  $p < 0.05$  by Tukey's post-hoc test.

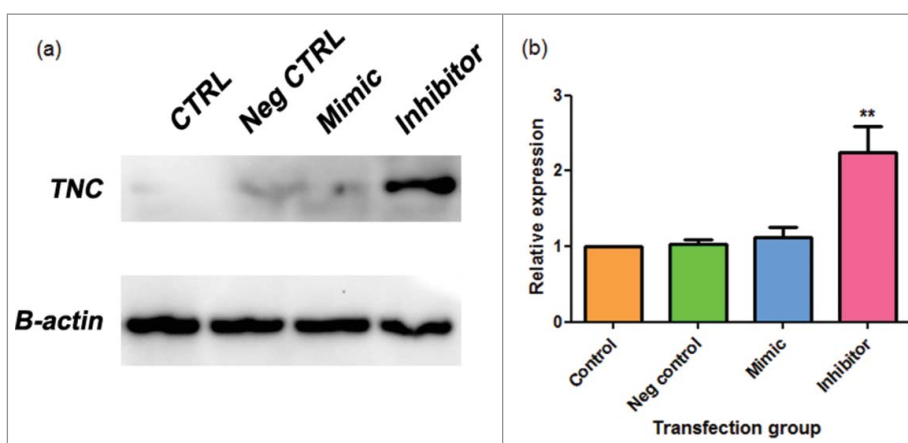


**Figure 7.** a-b. miR-335 inhibitor elevates TNC expression in MDA-MB-231 cells. (a) Sample western blot photographs for Tenascin C (TNC) and control beta-actin (B-actin) as shown on Image Lab. (b) Combined western blot data from Image Lab calculations. Data are expressed as means  $\pm$  SEM and are a combination of 3 experiments. MDA-MB-231 were transfected with a mirVana<sup>TM</sup> negative control 1 (neg control), miR-335 mimic, or miR-335 inhibitor. Samples were analyzed by western blot. Significance is represented by \*\* for p-value < 0.01 by Tukey's post-hoc test.

AHCC was particularly effective on the MDA-MB-231 triple negative cells (with no observed toxicity up to 8 mg/ml) (Fig. 1a-d). TNBC accounts for 10–20% of diagnosed breast cancers in women globally and has the highest recurrence rate of breast cancer subtypes because it lacks targeted therapies<sup>48–50</sup> TNBC is currently treated by radiation, surgery, and chemotherapies like paclitaxel. Paclitaxel is a taxane, which creates aberrant mitotic spindles,<sup>51</sup> but this mechanism does not allow for the targeting of CSCs and may even increase their number rather than reduce it.<sup>52</sup> When studying the epigenetic mechanisms underscoring the effects of AHCC on the MDA-MB-231 cells, we found important microRNAs to be involved in the potential inhibitory activity of AHCC against FESPP. By microRNA profiling, we have shown that several miRNAs, some of which are associated with different clinical-pathological characteristics of breast cancer, such as stemness, invasion and chemoresistance, could be differentially expressed after AHCC administration. For example, miRNAs miR-92a, miR-181a, miR-183\*, miR-335, miR-497, miR-500a, miR-720, and miR-1285<sup>53–60</sup> (Fig. 5). The main purpose of this profiling was to choose a target of interest and we elected to further study the particular role of AHCC on tumor suppressor mir-335 for its known involvement in breast cancer

metastasis and stem cell maintenance.<sup>56,61,62</sup> Confirming miRNA profiling results, the RT-qPCR analysis showed that AHCC significantly upregulated the expression of miR-335 in MDA-MB-231 cell culture (Fig. 6).

MiR-335 suppresses metastasis and migration via targeting protein pathways, such as that of the progenitor cell transcription factor SOX4 and extracellular matrix component tenascin C (TNC).<sup>61</sup> Several studies have previously linked miR-335 with TNC in cancer, which is also important in breast cancer metastasis and stem cell maintenance (149,156,201). Further, TNC might be involved with the anti-tumoral effects of AHCC through shared immune system targets. TNC inhibits cytotoxic T cell (CTL) activity<sup>63</sup> and AHCC increases it,<sup>7</sup> which could influence CSC immune evasiveness and resistance. Therefore, AHCC may increase CTL activity by inhibiting TNC through miR-335 upregulation, and possibly by targeting other miRNAs.

TNC protein expression was found to be increased in the presence of the miR-335 inhibitor, but it was not affected by the mirVana<sup>TM</sup> miR-335 mimic (Fig. 7a-b). One explanation for the ineffective mimic could be timing. In a study examining the effects of miR-335 transfection on hepatic stellate cells,

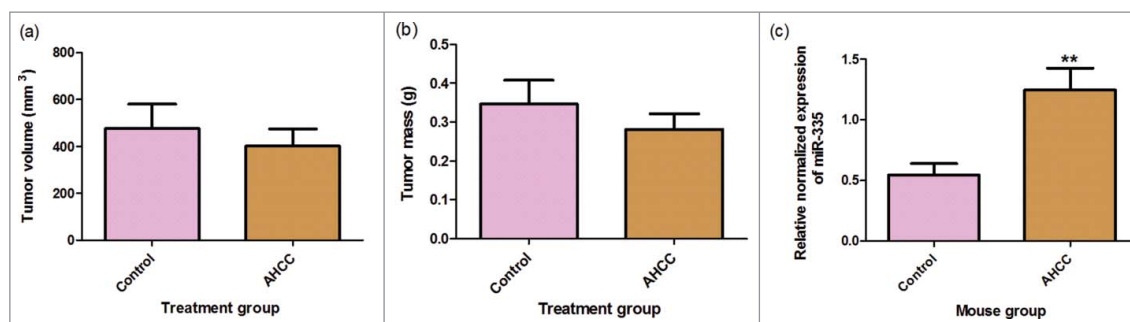


**Figure 8.** a-c. Mouse tumor measurements and miR-335 expression. (a) Mouse inner tumor volume. (b) Mouse tumor mass. Data are presented as mean  $\pm$  SEM. Tumor volume was calculated by the equation  $0.5 \times d^2 \times D$  where d is the smaller measured diameter and D is the larger measured diameter. Mice were gavaged for 2 weeks, injected with 4T1 cancer cells, and gavaged again for 18–23 days following injection. Tumors were extracted from mice following gavage period. The means were calculated with eleven treatment mice and nine control mice. (c) Change in miR-335 expression in mice gavaged with AHCC. Mice were gavaged with 1g/kg/day AHCC in 1% sucrose water or with 1% sucrose water (control). After 2 weeks of gavage, mice were injected with 4T1 cells and sacrificed 18–21 days following. Tumors were minced and digested for RT-qPCR analysis. Data are presented as mean  $\pm$  SEM. These are the results of two RT-qPCR runs with a total of 8 mice in the control group and 9 mice in the AHCC group. Quartile outliers were removed and \*\* indicates a significance of p-value < 0.01 by Tukey's post-hoc test.

TNC protein expression was not examined by western blot until 6 days after transfection, however, we extracted at 48 hours.<sup>64</sup> Nevertheless, other studies have found that a higher miR-335 presence lowers TNC luciferase activity and expression, and inhibits normal breast mammosphere growth.<sup>38,61</sup> Thus, both our study and the literature suggest that miR-335 negatively influences TNC and that both miR-335 and its target may play an important role in CSC regulation.

In order to validate the effect of AHCC in an *in vivo* setting, we used the breast cancer cell model previously established in our lab.<sup>65</sup> Although we were not able to see a significant difference in tumor growth with the oral gavage of AHCC, there was a downward trend. One explanation could be due to the dosage used. In this study, the dosage used was 1 g/kg/day which was the most common in the literature, however, doses in the literature for mice and rats ranged from 100 mg/kg/day to 12.5 g/kg/day and typically AHCC was combined with a chemotherapy agent.<sup>5,7,66–68</sup> Therefore, we cannot establish causation between AHCC and 4T1 tumor growth. However, it is reported in the literature that anti-tumoral mechanisms might target cellular pathways without directly affecting tumoral growth.<sup>69</sup> Importantly, there was an increased miR-335 expression in the AHCC mouse tumor samples compared to the controls (Fig. 8a-c). This suggests that AHCC also targets miR-335 *in vivo*. Previous animal studies with miR-335 have shown that it prevents breast cancer metastasis to the lungs and bones in mice after the injection of MDA-MB-231 into mice.<sup>61</sup>

## Conclusion

AHCC is a promising natural product for the complementary treatment of TNBC, previously shown to improve side effects caused by chemotherapy in breast cancer patients.<sup>3</sup> This study demonstrated that AHCC has a strong relationship with miR-335 pathways in different biological settings and that it could possibly target the oncogenic protein Tenascin C through miR-335 in a triple negative cell line. Overall, these findings suggest that AHCC effectively targets FESPP, making it an intriguing natural product for further research endeavors.

## Conflict of interest

Dr. Kohei Homma and Dr. Hiroshi Nishioka are employees of Amino Up Chemical Co., Ltd. All other co-authors have no financial interest in the company.

## Disclosure statement

The project received financial support from the AHCC Research Association. Dr. Kohei Homma and Dr. Hiroshi Nishioka are employees of Amino Up Chemical Co., Ltd. All other co-authors have no financial interest in the company.

## Acknowledgments

This study was financially possible by contributions from the AHCC Research Association and the Canadian Institutes of Health Research (CIHR). We would also like to thank Dr. Hector Hernandez-Vargas for his support and guidance with miRNA analysis. Finally, we would like to thank William Limoges for his technical assistance.

## References

- Villarini A, Pasanisi P, Traina A, Mano MP, Bonanni B, Panico S, Scipioni C, Galasso R, Paduos A, Simeoni M, et al. Lifestyle and breast cancer recurrences: the DIANA-5 trial. *Tumori*. 2012;98:1-18. PMID:22495696
- Cowawintaweevat S, Manoromana S, Sriplung H, Khuhaprema T, Tongtawe P, Tapchaisri P, Tapchaisri P, Chaicumpa W. Prognostic Improvement of patients with advanced liver cancer after Active Hexose Correlated Compound (AHCC) treatment. *Asian Pac J Allergy Immunol*. 2010;24:33-45.
- Hangai S, Iwase S, Kawaguchi T, Kogure Y, Miyaji T, Matsunaga T, Nagumo Y, Yamaguchi T. Effect of active hexose-correlated compound in women receiving adjuvant chemotherapy for breast cancer: a retrospective study. *J Altern Complement Med N. Y. N.* 2013;19:905-10. doi:10.1089/acm.2012.0914
- Turner J, Chaudhary U. Dramatic prostate-specific antigen response with activated hemicellulose compound in metastatic castration-resistant prostate cancer. *Anticancer Drugs*. 2009;20:215-6. doi:10.1097/CAD.0b013e3283163c26. PMID:19104437
- Hirose A, Sato E, Fujii H, Sun B, Nishioka H, Aruoma OI. The influence of active hexose correlated compound (AHCC) on cisplatin-evoked chemotherapeutic and side effects in tumor-bearing mice. *Toxicol Appl Pharmacol*. 2007;222:152-8. doi:10.1016/j.taap.2007.03.031. PMID:17555784
- Okuyama T, Yoshigai E, Ikeya Y, Nishizawa M. Active Hexose Correlated Compound extends the lifespan and increases the thermotolerance of Nematodes. *Research Gate*. 2013;3:166-82.
- Ritz BW, Nogusa S, Ackerman EA, Gardner EM. Supplementation with Active Hexose Correlated Compound increases the innate immune response of young mice to primary influenza infection. *J Nutr*. 2006;136:2868-73. PMID:17056815
- Gao Y, Zhang D, Sun B, Fujii H, Kosuna K-I, Yin Z. Active hexose correlated compound enhances tumor surveillance through regulating both innate and adaptive immune responses. *Cancer Immunol Immunother*. 2006;55:1258-66. doi:10.1007/s00262-005-0111-9. PMID:16362410
- Daddaoua A, Martínez-Plata E, López-Posadas R, Vieites JM, González M, Requena P, Zarzuelo A, Suárez MD, de Medina FS, Martínez-Augustín O. Active Hexose Correlated Compound acts as a prebiotic and is antiinflammatory in rats with hapten-induced colitis. *J Nutr*. 2007;137:1222-8. PMID:17449585
- Lee HE, Kim JH, Kim YJ, Choi SY, Kim S-W, Kang E, Chung IY, Kim IA, Kim EJ, Choi Y, et al. An increase in cancer stem cell population after primary systemic therapy is a poor prognostic factor in breast cancer. *Br J Cancer*. 2011;104:1730-8. doi:10.1038/bjc.2011.159. PMID:21559013
- Korkaya H, Liu S, Wicha MS. Regulation of cancer stem cells by cytokine networks: attacking cancer's inflammatory roots. *Clin. Cancer Res*. 2011;17:6125-9. doi:10.1158/1078-0432.CCR-10-2743. PMID:21685479
- Iliopoulos D, Polytaichou C, Hatzia Apostolou M, Kottakis F, Maroulakou IG, Struhl K, Tschlis PN. MicroRNAs differentially regulated by Akt isoforms control EMT and stem cell renewal in cancer cells. *Sci Signal*. 2009;2:ra62. doi:10.1126/scisignal.2000356. PMID:19825827
- Wicha MS, Liu S, Dontu G. Cancer stem cells: An old idea—A paradigm shift. *Cancer Res*. 2006;66:1883-90. doi:10.1158/0008-5472.CAN-05-3153. PMID:16488983
- Wicha MS. Cancer stem cells and metastasis: lethal seeds. *Clin Cancer Res*. 2006;12:5606-7. doi:10.1158/1078-0432.CCR-06-1537. PMID:17020960
- Lee H-S, Herceg Z. The epigenome and cancer prevention: A complex story of dietary supplementation. *Cancer Lett*. 2014;342:275-84. doi:10.1016/j.canlet.2012.01.021. PMID:22266189
- Dontu G, Al-Hajj M, Abdallah WM, Clarke MF, Wicha MS. Stem cells in normal breast development and breast cancer. *Cell Prolif*. 2003;36 Suppl 1:59-72. doi:10.1046/j.1365-2184.36.s.1.6.x. PMID:14521516
- Wicha MS. Identification of murine mammary stem cells: implications for studies of mammary development and carcinogenesis. *Breast Cancer Res BCR*. 2006;8:109. doi:10.1186/bcr1540. PMID:16934104
- Al-Hajj M, Wicha MS, Benito-Hernandez A, Morrison SJ, Clarke MF. Prospective identification of tumorigenic breast cancer cells. *Proc Natl Acad Sci U. S. A.* 2003;100:3983-8. doi:10.1073/pnas.0530291100. PMID:12629218



19. Han M, Liu M, Wang Y, Chen X, Xu J, Sun Y, Zhao L, Qu H, Fan Y, Wu C. Antagonism of miR-21 reverses Epithelial-Mesenchymal Transition and cancer stem cell phenotype through AKT/ERK1/2 inactivation by targeting PTEN. *PLoS One*. 2012;7:1-11.
20. Ellis SL, Heazlewood SY, Williams B, Reitsma AJ, Grassinger J, Borg J, Heazlewood CK, Chidgey AP, Nilsson SK. The role of Tenascin C in the lymphoid progenitor cell niche. *Exp Hematol*. 2013;41:1050-61. doi:10.1016/j.exphem.2013.09.009. PMID:24084079
21. Oskarsson T, Acharyya S, Zhang XH-F, Vanharanta S, Tavazoie SF, Morris PG, Downey RJ, Manova-Todorova K, Brogi E, Massagué J. Breast cancer cells produce tenascin C as a metastatic niche component to colonize the lungs. *Nat Med*. 2011;17:867-74. doi:10.1038/nm.2379. PMID:21706029
22. Midwood KS, Orend G. The role of tenascin-C in tissue injury and tumorigenesis. *J Cell Commun Signal*. 2009;3:287-310. doi:10.1007/s12079-009-0075-1. PMID:19838819
23. Ruiz C, Huang W, Hegi ME, Lange K, Hamou M-F, Fluri E, Oakeley EJ, Chiquet-Ehrismann R, Orend G. Growth promoting signaling by tenascin-C [corrected]. *Cancer Res*. 2004;64:7377-85. doi:10.1158/0008-5472.CAN-04-1234. PMID:15492259
24. Tamaoki M, Imanaka-Yoshida K, Yokoyama K, Nishioka T, Inada H, Hiroe M, Sakakura T, Yoshida T. Tenascin-C regulates recruitment of myofibroblasts during tissue repair after myocardial injury. *Am J Pathol*. 2005;167:71-80. doi:10.1016/S0002-9440(10)62954-9. PMID:15972953
25. Sever M, Mammadov B, Guler MO, Tekinay AB. Tenascin-C mimetic Peptide nanofibers direct stem cell differentiation to osteogenic lineage. *Biomacromolecules*. 2014;15:4480-7. doi:10.1021/bm501271x. PMID:25343209
26. Goh FG, Piccinini AM, Krausgruber T, Udalova IA, Midwood KS. Transcriptional regulation of the endogenous danger signal tenascin-C: a novel autocrine loop in inflammation. *J Immunol Baltim Md 1950*. 2010;184:2655-62.
27. Hendaoui I, Tucker RP, Zingg D, Bichet S, Schittny J, Chiquet-Ehrismann R. Tenascin-C is required for normal Wnt/ $\beta$ -catenin signaling in the whisker follicle stem cell niche. *Matrix Biol J Int Soc Matrix Biol*. 2014;40:46-53. doi:10.1016/j.matbio.2014.08.017
28. Bellone M, Caputo S, Jachetti E. Immunosuppression via Tenascin-C. *Oncoscience*. 2015;2:667-8. doi:10.18632/oncoscience.210. PMID:26425650
29. Liu C, Tang DG. MicroRNA regulation of cancer stem cells. *Cancer Res*. 2011;71:5950-4. doi:10.1158/0008-5472.CAN-11-1035. PMID:21917736
30. Bao B, Li Y, Ahmad A, Azmi AS, Bao G, Ali S, Banerjee S, Kong D, Sarkar FH. Targeting CSC-related miRNAs for cancer therapy by natural agents. *Curr Drug Targets*. 2012;13:1858-68. doi:10.2174/138945012804545515. PMID:23140295
31. Shi B, Sepp-Lorenzino L, Prisco M, Linsley P, deAngelis T, Baserga R. Micro RNA 145 targets the insulin receptor substrate-1 and inhibits the growth of colon cancer cells. *J Biol Chem*. 2007;282:32582-90. doi:10.1074/jbc.M702806200. PMID:17827156
32. Hatfield S, Ruohola-Baker H. microRNA and stem cell function. *Cell Tissue Res*. 2008;331:57-66. doi:10.1007/s00441-007-0530-3. PMID:17987317
33. Erturk E, Cecener G, Egeli U, Tunca B, Tezcan G, Gokgoz S, Tolunay S, Tasdelen I. Expression status of let-7a and miR-335 among breast tumors in patients with and without germ-line BRCA mutations. *Mol Cell Biochem*. 2014;395:77-88. doi:10.1007/s11010-014-2113-4. PMID:24942235
34. Gao Y, Zeng F, Wu J-Y, Li H-Y, Fan J-J, Mai L, Zhang J, Ma DM, Li Y, Song FZ. MiR-335 inhibits migration of breast cancer cells through targeting oncoprotein c-Met. *Tumour Biol*. 2015;36:2875-83. doi:10.1007/s13277-014-2917-6. PMID:25492484
35. Meng Y, Zou Q, Liu T, Cai X, Huang Y, Pan J. microRNA-335 inhibits proliferation, cell-cycle progression, colony formation, and invasion via targeting PAX6 in breast cancer cells. *Mol Med Rep*. 2015;11:379-85. doi:10.3892/mmr.2014.2684. PMID:25323813
36. Vimalraj S, Miranda PJ, Ramyakrishna B, Selvamurugan N. Regulation of breast cancer and bone metastasis by microRNAs. *Dis Markers*. 2013;35:369-87. doi:10.1155/2013/451248. PMID:24191129
37. Scarola M, Schoeftner S, Schneider C, Benetti R. miR-335 directly targets Rb1 (pRb/p105) in a proximal connection to p53-dependent stress response. *Cancer Res*. 2010;70:6925-33. doi:10.1158/0008-5472.CAN-10-0141. PMID:20713524
38. Polyarchou C, Iliopoulos D, Struhl K. An integrated transcriptional regulatory circuit that reinforces the breast cancer stem cell state. *Proc Natl Acad Sci U S A*. 2012;109:14470-5. doi:10.1073/pnas.1212811109. PMID:22908280
39. Pulaski BA, Ostrand-Rosenberg S. Mouse 4T1 breast tumor model. Coligan JE, editor. *Curr Protoc Immunol*. New Jersey (USA): John Wiley & Sons Inc; 2001. 39 Suppl. 20.2.20.1-20.2.16
40. Bolstad BM, Irizarry RA, Astrand M, Speed TP. A comparison of normalization methods for high density oligonucleotide array data based on variance and bias. *Bioinforma Oxf Engl*. 2003;19:185-93. doi:10.1093/bioinformatics/19.2.185
41. Manuel Iglesias J, Belouqui I, Garcia-Garcia F, Leis O, Vazquez-Martin A, Eguara A, Cufi S, Pavin A, Menendez JA, Dopazo J, et al. Mammotome formation in breast carcinoma cell lines depends upon expression of E-cadherin. *PLoS One*. 2013;8:e77281. doi:10.1371/journal.pone.0077281. PMID:24124614
42. Collina F, Di Bonito M, Li Bergolis V, De Laurentiis M, Vitagliano C, Cerrone M, Nuzzo F, Cantile M, Botti G. Prognostic value of cancer stem cells markers in triple-negative breast cancer. *BioMed Res Int*. 2015;2015:158682. doi:10.1155/2015/158682. PMID:26504780
43. Cao Z, Chen X, Lan L, Zhang Z, Du J, Liao L. Active hexose correlated compound potentiates the antitumor effects of low-dose 5-fluorouracil through modulation of immune function in hepatoma 22 tumor-bearing mice. *Nutr Res Pract*. 2015;9:129-36. doi:10.4162/nrp.2015.9.2.129. PMID:25861418
44. Matsushita K, Kuramitsu Y, Ohno Y, Obara M, Kobayashi M, Li YQ, Hosokawa M. Combination therapy of active hexose correlated compound plus UFT significantly reduces the metastasis of rat mammary adenocarcinoma. *Anticancer Drugs*. 1998;9:343-50. doi:10.1097/00001813-199804000-00008. PMID:9635925
45. Schwarz-Cruz Y, Celis A, Espinosa M, Maldonado V, Melendez-Zajgla J. Advances in the knowledge of breast cancer stem cells. A Review *Histol Histopathol*. 2015;31(6):601-12. doi:10.14670/HH-11-718.
46. Nawata J, Kuramitsu Y, Wang Y, Kitagawa T, Tokuda K, Baron B, Akada J, Suenaga S, Kaino S, Maehara S, et al. Active hexose-correlated compound down-regulates sex-determining region Y-box 2 of pancreatic cancer cells. *Anticancer Res*. 2014;34:4807-11. PMID:25202061
47. Duru N, Gernapudi R, Eades G, Eckert R, Zhou Q. Epigenetic Regulation of miRNAs and breast cancer stem cells. *Curr Pharmacol Rep*. 2015;1:161-9. doi:10.1007/s40495-015-0022-1. PMID:26052481
48. Dent R, Trudeau M, Pritchard KI, Hanna WM, Kahn HK, Sawka CA, Lickley LA, Rawlinson E, Sun P, Narod SA. Triple-negative breast cancer: clinical features and patterns of recurrence. *Clin Cancer Res Off J Am Assoc Cancer Res*. 2007;13:4429-34. doi:10.1158/1078-0432.CCR-06-3045
49. Martin HL, Smith L, Tomlinson DC. Multidrug-resistant breast cancer: current perspectives. *Breast Cancer Targets Ther*. 2014;6:1-13.
50. Boyle P. Triple-negative breast cancer: epidemiological considerations and recommendations. *Ann Oncol Off J Eur Soc Med Oncol ESMO*. 2012;23 Suppl 6:vi7-12. doi:10.1093/annonc/mds187
51. Paclitaxel (Taxol, Onxal) Chemotherapy Drug Information [Internet]. [cited 2016 Apr 3]. Available from: <http://chemocare.com/chemotherapy/drug-info/Paclitaxel.aspx>
52. Larzabal L, El-Nikhely N, Redrado M, Seeger W, Savai R, Calvo A. Differential effects of Drugs Targeting Cancer Stem Cell (CSC) and Non-CSC populations on lung primary tumors and metastasis. *Plos One*. 2013;8:e79798. doi:10.1371/journal.pone.0079798. PMID:24278179
53. Nilsson S, Möller C, Jirström K, Lee A, Busch S, Lamb R, Landberg G. Downregulation of miR-92a is associated with aggressive breast cancer features and increased tumour macrophage infiltration. *PLoS One*. 2012;7:e36051. doi:10.1371/journal.pone.0036051. PMID:22563438
54. Niu J, Xue A, Chi Y, Xue J, Wang W, Zhao Z, et al. Induction of miRNA-181a by genotoxic treatments promotes chemotherapeutic resistance and metastasis in breast cancer. *Oncogene*. 2015;35(10):1302-1313. doi:10.1038/onc.2015.189.
55. Lowery AJ, Miller N, Dwyer RM, Kerin MJ. Dysregulated miR-183 inhibits migration in breast cancer cells. *BMC Cancer*. 2010;10:502. doi:10.1186/1471-2407-10-502. PMID:20858276
56. Tomé M, López-Romero P, Albo C, Sepúlveda JC, Fernández-Gutiérrez B, Dopazo A, Bernad A, González MA. miR-335 orchestrates cell

- proliferation, migration and differentiation in human mesenchymal stem cells. *Cell Death Differ.* 2011;18:985-95. doi:10.1038/cdd.2010.167. PMID:21164520
57. Wu Z, Li X, Cai X, Huang C, Zheng M. miR-497 inhibits epithelial mesenchymal transition in breast carcinoma by targeting Slug. *Tumour Biol J Int Soc Oncodevelopmental Biol Med.* 2015;37(6), 7939-50. doi:10.1007/s13277-015-4665-7.
58. Janssen EAM, Slewa A, Gudlaugsson E, Jonsdottir K, Skaland I, Söiland H, Baak JP. Biologic profiling of lymph node negative breast cancers by means of microRNA expression. *Mod Pathol.* 2010;23:1567-76. doi:10.1038/modpathol.2010.177. PMID:20818337
59. Li L-Z, Zhang CZ, Liu L-L, Yi C, Lu S-X, Zhou X, Zhang ZJ, Peng YH, Yang YZ, Yun JP. miR-720 inhibits tumor invasion and migration in breast cancer by targeting TWIST1. *Carcinogenesis.* 2014;35:469-78. doi:10.1093/carcin/bgt330. PMID:24085799
60. Gonul O, Aydin HH, Kalmis E, Kayalar H, Ozkaya AB, Atay S, Ak H. Effects of *Ganoderma lucidum* (higher basidiomycetes) extracts on the miRNA profile and telomerase activity of the MCF-7 breast cancer cell line. *Int J Med Mushrooms.* 2015;17:231-9. doi:10.1615/IntJMedMushrooms.v17.i3.30. PMID:25954907
61. Tavazoie SF, Alarcón C, Oskarsson T, Padua D, Wang Q, Bos PD, Gerald WL, Massagué J. Endogenous human microRNAs that suppress breast cancer metastasis. *Nature.* 2008;451:147-52. doi:10.1038/nature06487. PMID:18185580
62. Tomé M, Sepúlveda JC, Delgado M, Andrades JA, Campisi J, González MA, Bernad A. miR-335 correlates with senescence/aging in human mesenchymal stem cells and inhibits their therapeutic actions through inhibition of AP-1 activity. *Stem Cells Dayt. Ohio.* 2014;32:2229-44. doi:10.1002/stem.1699
63. Jachetti E, Caputo S, Mazzoleni S, Brambillasca CS, Parigi SM, Grioni M, Piras IS, Restuccia U, Calcinotto A, Freschi M, et al. Tenascin-C protects cancer stem-like cells from immune surveillance by arresting T-cell activation. *Cancer Res.* 2015;75:2095-108. doi:10.1158/0008-5472.CAN-14-2346. PMID:25808872
64. Chen C, Wu C-Q, Zhang Z-Q, Yao D-K, Zhu L. Loss of expression of miR-335 is implicated in hepatic stellate cell migration and activation. *Exp Cell Res.* 2011;317:1714-25. doi:10.1016/j.yexcr.2011.05.001. PMID:21586285
65. Vuong T, Matar C, Ramassamy C, Haddad PS. Biotransformed blueberry juice protects neurons from hydrogen peroxide-induced oxidative stress and mitogen-activated protein kinase pathway alterations. *Br J Nutr.* 2010;104:656-63. doi:10.1017/S0007114510001170. PMID:20459875
66. Aviles H, O'Donnell P, Orshal J, Fujii H, Sun B, Sonnenfeld G. Active hexose correlated compound activates immune function to decrease bacterial load in a murine model of intramuscular infection. *Am J Surg.* 2008;195:537-45. doi:10.1016/j.amjsurg.2007.05.045. PMID:18304499
67. Aviles H, Belay T, Fountain K, Vance M, Sun B, Sonnenfeld G. Active hexose correlated compound enhances resistance to *Klebsiella pneumoniae* infection in mice in the hindlimb-unloading model of spaceflight conditions. *J Appl Physiol Bethesda Md* 1985. 2003;95:491-6.
68. Fujii H, Nishioka N, Simon RR, Kaur R, Lynch B, Roberts A. Genotoxicity and subchronic toxicity evaluation of Active Hexose Correlated Compound (AHCC). *Regul Toxicol Pharmacol.* 2011;59:237-50. doi:10.1016/j.yrtph.2010.10.006. PMID:20951179
69. Nagakawa H, Shimozato O, Yu L, Takiguchi Y, Tatsumi K, Kuriyama T, Tagawa M. Expression of interleukin-22 in murine carcinoma cells did not influence tumour growth *in vivo* but did improve survival of the inoculated hosts. *Scand J Immunol.* 2004;60:449-54. doi:10.1111/j.0300-9475.2004.01504.x. PMID:15541036